Molecular Constitutive Model for Entangled Polymer Nanocomposites

CATALIN R. PICU[1]*, ALIREZA S. SARVESTANI[2]*, LIVIU IULIAN PALADE[3]*

[1] Department of Mechanical, Aerospace and Nuclear Engineering, Rensselaer Polytechnic Institute, Troy, NY 12180, USA.

[2] University of Maine, Department of Mechanical Engineering and Graduate School of Biomedical Sciences, Orono, ME 04469, USA.

[3] Université de Lyon, CNRS, Institut Camille Jordan UMR 5208, INSA-Lyon, Pôle de Mathématiques, Bât. Léonard de Vinci No. 401, 21 Avenue Jean Capelle, F-69621 Villeurbanne, France.

A molecular rheological model for amorphous homopolymers filled with nanoparticles is presented. The fillers are non-agglomerated and interact energetically with the polymers. The model applies to situations in which the polymer-filler affinity is relatively weak. The essential physics represented in the model includes chain reptation, the slowing down of diffusion due to energetic interactions of polymers and fillers, chain stretch, and contour length fluctuations. The model is based on insight obtained from extensive simulations of the structure and dynamics of these systems. The chain population is composed of free, dangling and bridging chains, i.e. those that at given time do not contact fillers, contact one filler or multiple fillers, respectively. As the system evolves, a representative chain switches randomly between these categories. The representative chain reptates only when free, while contour length fluctuations are performed at all times. Relaxation is controlled by both tube renewal and the process of chain attachment/detachment to/from the filler surface. The second process modulates the first, leading to a relaxation with two characteristic times, in agreement with experimental observations. The parameters entering the model can be calibrated based on the rheology of the neat polymer and based on results from simulations of the respective filled system.

Keywords: rheology of polymer nano-composites; reptation; contour length fluctuation; tube renewal

Polymer nanocomposites represent a new class of materials of significant current interest. The attention they receive is due to the hope that novel combinations of properties can be obtained by mixing polymers with nano-objects. The key requirement is that the fillers have dimensions similar to those of the polymeric chains. The chain size, e.g. the radius of gyration, sets an internal length scale for the material. The nano-object dimensions define another (or several) length scale. The interplay of these length scales influences the physics underlying the material behavior. Indeed, many recent experimental studies suggest that material properties of the polymer change upon addition of a small volume fraction of nanometer sized filler particles [e.g. Wei *et al.* (2004) [41]; Zhang and Archer (2002 [39], 2004 [40]); Sternstein and Zhu (2002) [36]; Ozisik *et al.* (2005) [21]]. For example, the viscosity and the low frequency storage and loss moduli increase significantly compared to the neat polymer, and a relatively brittle polymer like PMMA transforms into a ductile one upon mixing with nanoparticles [Ng et al. (1999) [20]].

However, not all researchers report improvements in material properties. In fact, one may find multiple reports referring to the same material system that contradict each other. These discrepancies are attributed, in part, to two reasons. If the fillers are poorly dispersed, one recovers the properties expected for the equivalent micro-composite of similar filler volume fraction. If fillers are well dispersed in the matrix, but the polymer-filler interaction is not controlled, one may or may not obtain the desired enhancement in properties. Generally, just as in the case of regular particulate composites, reinforcement is obtained if the interface is well bonded. A weak interface assists cavitation, which improves ductility and fracture toughness.

These considerations indicate that gaining control over material processing is crucial. This can be done either by an experimental trial and error procedure, or by a combination of modeling and simulation and experiments. In order to advance along the second path, developing constitutive representations of the material behavior that incorporate the small scale physics is important. Such models offer the possibility to optimize with respect to nanoscale parameters both material response and material processing. This is the objective of the present work. Specifically, a constitutive formulation is being presented for the mechanical response of polymer nanocomposite melts. The composites considered here are composed from linear polymers and nanoparticles. The fillers are well dispersed in the matrix.

The development of rheological molecular models for neat polymers has a long history. The most successful models available to date are those based on the tube concept proposed by de Gennes and developed by Doi and Edwards and other workers [Doi and Edwards (1986) [6]; Bird *et al.* (1987) [1]]. In this class of models, the major relaxation mechanisms are the reptation of the chain within the mesh of entanglements created by the surrounding chains, the fluctuations of the tube length and the release of topological constraints due to the motion of surrounding chains. Of these, the first two have been treated in the

* *email: picuc@rpi.edu; alireza.sarvestani@umit.maine.edu, liviu-iulian.palade@insa-lyon.fr*

mean field sense and led to models that reproduce the main features of the rheology [e.g. Mead and Leal (1995) [15]; Mead et al. (1995 [16], 1998) [17]]. The third effect is more difficult to be predicted within the mean field approximation of chain dynamics and various methods have been developed to cope with this difficulty [Ianniruberto and Marrucci (2000 [11], 2001 [12]); Milner et al. (2001) [19]; Graham et al. (2003) [9]; Shima et al. (2003) [33]]. The linear rheology of monodisperse neat melts is well represented by the current models. The non-linear aspects of the problem are less well described. Accounting for chain polydispersity poses major problems, as the controlling physics in such systems is related to non-linear effects of the constraint release type.

The rheology of mixtures of linear monodisperse polymers and nanofillers is comparatively much more difficult to model. The problem was addressed in the context of short, unentangled polymers [Sarvestani and Picu (2004) [30]] and polymers close to the overlap threshold [Sarvestani and Picu (2005) [31]]. In the first case, the dominant response comes from the transient network of chains that bridge fillers. In the second, in addition to the secondary network effect [Reichert et al. (1993) [28]], one has a slowing down of dynamics due to the enthalpic interactions between chains and fillers.

In this work, heavily entangled systems are considered. In this case, the physics is dominated by the confinement of the representative chain in the "tube" and by its interaction with fillers. The polymer-filler interaction is considered relatively weak, such that the probability of chain detachment (and, potentially, reattachment) on a time scale comparable with the Rouse time of the respective chain is smaller, but close to one. As with all other models of the rheology of neat polymers, one has to make assumptions about the dominant physics and attempt to capture it in tractable analytical forms. The key aspects of the physics considered here are presented in Section 2. The model is presented in Section 3, while in Section 4 it is studied how these assumptions influence the model behavior. A qualitative comparison with experimental data is presented in the closing section.

The material and overview of simulation data

The system considered here is a mixture of linear monodisperse homopolymers and nanoparticles. The fillers are spherical, of identical diameter and are impenetrable for the polymeric chains. Their deformation during flow of the suspension is negligible. This system is representative for materials of the type tested by Zhang and Archer (2004) [39], Sternstein and Zhu (2002) [36] and Zhu et al. (2005) [40], in which fillers are properly dispersed in the matrix (limited filler agglomeration).

The filler radius, R, is smaller or similar to the chain radius of gyration, R_g, in the neat bulk. Situations in which fillers are much larger than R_g may also be represented. This is the limit of regular polymer composites, in which the filler size is orders of magnitude larger than the size of the chains. However, these cases are considered less interesting on the basis of the experimental evidence discussed in the Introduction showing that enhanced material properties are obtained when R and R_g are comparable.

The molecular weight of the chains is assumed to be much larger than the entanglement molecular weight. The length of the entanglement segment is denoted by a, while the number of such segments in a chain is denoted by N. These quantities are those inferred for the neat bulk polymer from macroscopic experiments or from atomistic/molecular simulations. Here it is assumed that a remains unchanged in presence of nanoparticles, an issue which is discussed further below.

The model is based to a large extent on insight regarding the structure and dynamics of this system in equilibrium obtained by atomistic simulations [Ozmusul and Picu (2002) [22]; Picu and Ozmusul (2003) [26]; Dionne *et al.* (2005) [3]]. A brief review of the results obtained from these studies is necessary. The key parameters are those defining the geometry: the filler radius, R, the average wall-to-wall distance, d, the chain radius of gyration in the neat polymer, R_g, and the parameter w describing the polymer-filler affinity. w represents the ratio of the depth of the potential well of the polymer-filler vs. polymer-polymer interactions and includes effects related to surface heterogeneities (geometric and chemical) which have been shown to be important in this context [Smith et al. (2003) [34]]. w can be also regarded as an internal parameter describing the way polymers interact with fillers and controlling the life-time of polymer-filler contacts. Neutral polymer-filler interactions are represented by w = 1. Weak bonding corresponds to $w \sim 4$, while strong H bonding corresponds to $w \sim 10$ and larger. These values are obtained by using as guideline the strength of various types of H bonds and the depth of the well of non-bonded interactions in coarse grained models of polyethylene, which is about 230 k_B [Clancy and Mattice (2001) [2]] (with k_B being the Boltzmann's constant).

The structure of this system can be characterized on multiple length scales. The smallest relevant scale is that of the Kuhn segment. If the polymer-filler interaction is purely repulsive (excluded volume), the cohesive interactions in the bulk polymer and the chain configurational entropy force retract the beads from the filler leading to a low density layer in the neighborhood of the filler surface. It has been conjectured that this effect assists cavitation [Ng et al. (1999) [20]]. Neutral and attractive (energetic) interactions prevent the formation of such depleted layer. Simulations also suggested that chain segments as well as entire chains gain preferential orientation in the vicinity of the filler surface. This is known in the literature on flat interfaces as a "docking transition" [Pakula (1991) [24]]. On the scale of the entire chain, it is observed that the chain semiaxes (eigenvalues of the gyration tensor) do not change in length as the center of mass of the chain approaches the filler, but the direction of the largest semiaxis (corresponding eigenvector) rotates in the direction tangential to the filler surface. The predominance of this transformation over that involving chain distortion can be understood considering that the variation in configurational entropy of the entire system associated with docking is much smaller than that associated with chain distortion. Interestingly, this result remains valid even for rather large polymer-filler affinities such as w = 12. For much larger w it is expected that the chains in the close neighborhood of the wall flatten out. This leads to the "passivation" of the filler surface, an increase of the effective filler diameter and to tethering of the chains in contact with the surface.

When the average wall-to-wall distance d is equal or smaller than $2R_g$, the probability that a chain contacts simultaneously more than one filler becomes non-negligible. Such chains form bridges between fillers; this leads to a polymer-mediated filler network. This network is transient in the sense that it is reshaped either by thermal fluctuations or by deformation.

The statistics of this "secondary network" was studied by means of simulations [Ozmusul et al. (2005) [23]]. It was observed that: a) the number of bridges per filler

increases fast as d decreases below $2R_g$, b) The chains forming bridges are not distorted compared to those in the neat polymer, rather they represent samples of the tail of the Gaussian end-end vector distribution in the neat system. c) Each filler carries a large number of dangling chains which are in contact with the respective filler only. The distribution of such dangling ends is very broad (dangling ends of length from 1 to N are present with almost equal probability). d) A representative contact between a filler and a chain rarely involves only one bead/Kuhn segment. The more common situation is when the chain forms a "train", i.e. a segment that snakes on the surface of the filler.

The chain dynamics is perturbed by the presence of fillers due to both the filler excluded volume effect (topological confinement), and due to the energetic polymer-filler interaction [Dionne *et al*. (2006) [4]]. The topological confinement affects the Rouse modes if $d < 1.2R_g$, while the slowing down effect due to the energetic interactions is present in all cases, provided $w > 2$. When w is sufficiently large to prevent chain detachment, the chains are essentially tethered to the filler surface. In this case, the relaxation of the remaining, free chains is slowed down due to their interaction with the dangling ends.

The lifetime of the chain-filler contacts was also studied by means of simulations [Smith et al. (2005) [35]; Dionne et al. (2006) [4]]. The attachment/detachment process is controlled by the local energetics and compressibility, the filler surface topology, and by the diffusive motion of the chains. The chains execute Rouse motion with an effective friction which depends on w. The relationship between the length of the attached segment (including the trains and the loops between trains) and the lifetime of the contact follows Rouse scaling. This relationship breaks down for strongly adsorbed chains having almost all beads attached to the filler.

The distribution of lifetimes is strongly skewed toward the short contact times and has a long tail in the range of long contact times. The average lifetime of the adsorption, t_{ad}, scales with the affinity w as $\exp(w/k_BT)$ reflecting the thermally activated nature of the detachment process (T represents the absolute temperature). This relation was inferred from models of dense systems (although compressibility was not accounted for in these studies). It must be observed that τ_{ad} increases very fast with w due to the exponential, which implies that even for modest w values, the chains appear tethered to the filler on time scales comparable to the relaxation of chains in the neat bulk. Other local details of the dynamics, including the rotation barriers and the effect of the nanoparticle surface roughness may affect τ_{ad}, but these effects were not studied in detail in the references cited.

The model

The rheological model presented below is based on these findings. At given time, the system contains fractions ϕ_0, ϕ_1 and ϕ_2 of free chains that contact no filler, dangling and bridging chains, respectively ($\phi_0 + \phi_1 + \phi_2 = 1$). It is assumed that the bridging chains contact no more than two fillers. A schematic representation of the three types of chains is shown in figure 1. Dangling chains are composed from two dangling segments of length N_1 and N_2, while bridging chains are composed of two dangling segments of length N_1 and N_2, and a bridging segment of length N_3 ($N_1+N_2+N_3+2=N$, with N being the number of entanglement segments of the monodisperse chains in the melt).

Relaxation in this system takes place by reptation, which is modulated by the chain-filler attachment/detachment process. Since the system is considered heavily entangled and τ_{ad} is not much higher than τ_R (τ_R is the longest Rouse relaxation time) Rouse relaxation is neglected.

We consider that a representative chain changes type in average every τ_{ad}, switching at random from one sub-population to another. The number of chains leaving a population in any given interval of time is equal to the number of chain entering that group, in order to maintain the fractions ϕ constant. Note that the probability of switching from free to bridging is much lower than that of switching from free to dangling and from dangling to bridging (and vice-versa), and the associated mean time should be on the order of τ_{ad}^2. This distinction is ignored in the numerical examples presented in Section 4.

Tube renewal takes place as in the neat system, by reptation and by contour length fluctuations. Reptation occurs only when the chain is free, while contour length fluctuations are performed at all times.

Here it is considered that the characteristic length scale of the reptation process, the tube diameter, a, is the same as in the neat system. Since only the free chains reptate, and these are located at some distance from the filler surface, the assumption seems plausible. Suggestions were made in the literature that a changes in the vicinity of a rigid wall [Ganesan and Pryamitsyn (2002) [8]]. It is clear that if the density at the wall is different than that in the bulk (excluding the usual packing fluctuations which are short ranged), the entanglement length should change. If the density is similar to that in the bulk, the answer is not obvious. If one uses the evaluation method for a based on packing considerations [Kavassalis and Noolandi (1988) [13]; Fetters et al. (1999) [7]], a change of a is expected simply based on topology; however, it is not clear that the method is transferable from the neat bulk polymer to the situation studied here. Simulations of equilibrium dynamics in large models employing chains significantly longer than the entanglement length indicate that the tube diameter computed as a mean over all the chains in the filled system, is identical to that in the neat polymer [Picu and Rakshit, (2007) [27]].

The fillers are considered to move affinely with the macro-deformation. If the filler-polymer interaction is attractive (the only situation of importance if reinforcement is desired) the situation is akin to that in networks. The fluctuations of a network node decrease in amplitude with the network coordination number. Here, the node is the filler and the "coordination" is equal to the number of bridges per filler which, in all cases of interest, is larger than 3. Since this "network" is not permanent, it should be assumed that the fillers perform random walks with a characteristic time on the order of τ_{ad}, i.e. much slower than both the beads and the chain centers of mass. Hence, the assumption of affinely moving fillers is based on the separation of time scales between the chain and filler diffusion processes.

The average lifetime of the chain-filler attachments τ_{ad} is considered to be larger than τ_R, the Rouse time of the entire chain. This corresponds to $w > 4$ [Dionne et al. (2006) [4]]. The basic concept on which the model stands, that of chains switching between the three sub-populations and modulating reptation, is expected to break down in the limit of $\tau_{ad} >> \tau_R$ (or large w), and hence the model should not apply in such situations. The attachment lifetime can be made a function of the chain stretch as in [Sarvestani and Picu (2005) [31]]. This would lead to significant shear

thinning in high rate flows. This effect is not considered here but can be included in the model.

The hydrodynamic interactions are neglected in this model both for polymers (melt state) and for fillers. Hence, the filler excluded volume plays no direct role in the model, i.e. fillers are similar to material points. Their presence is felt only through the interaction with the chains. The hydrodynamics of the fillers is expected to be important in high rate flows and at large filler volume fractions.

Reptation

Let us consider a representative chain of the system, which begins as a free chain and becomes at random dangling and bridging, or remains free. The transition probabilities are given by the respective fractions, ϕ_1 and ϕ_2. Let us assume that the transition takes place every τ_{ad}, with $\tau_{ad} > \tau_R$. The MSD (mean square displacement) of the free chain center of mass during a τ_{ad} period in the tube direction (1D diffusion) is given as in the neat bulk by

$$MSD(\tau_{ad}) = a^2 \frac{\bar{\tau}_{ad}}{N}, \qquad (1)$$

where $\bar{\tau}_{ad} = \tau_{ad}/\tau_R(a)$, and the notation $\tau_R(Ma)$ is used for the Rouse time of the segment of length Ma ($M > 1$), with $\tau_R(a)$ being the Rouse time of the entanglement segment of length a. The Rouse time of the whole chain is denoted as $\tau_R(Na)$. Here and in the following all time quantities are normalized by $\tau_R(a)$. A normalized quantity is denoted by an overbar.

While the chain is dangling or bridging, the MSD with respect to a given reference time $t = 0$ remains unchanged. Let us consider that the representative chain undergoes a random process of switching from one category to another, reptating only when free. For a realization of such random sequence (there are $\bar{t}/\bar{\tau}_{ad}+1$ switches up to time $\bar{t}$) one may write the total MSD at $\bar{t}$ as

$$MSD(\bar{t}) = a^2 \frac{\bar{\tau}_{ad}}{N} \prod_{j=1}^{\bar{t}/\bar{\tau}_{ad}} \left(\frac{(j+1)\bar{\tau}_{ad}}{j\bar{\tau}_{ad}} \right)^{q_j} \qquad (2)$$

where the power $q_j = 0$, if the chain is dangling or bridging, and $q_j = 1$ if the chain is free during the respective time interval $(j\bar{\tau}_{ad}, j\bar{\tau}_{ad} + \bar{\tau}_{ad})$. Note that, by ergodicity, $q_j = 1$ for a fraction ϕ_0 of all terms present in the product (2), such that $\langle q \rangle = \phi_0$.

The product in expression (2) appears when superimposing the contribution to MSD of the various time intervals $(j\bar{\tau}_{ad}, j\bar{\tau}_{ad} + \bar{\tau}_{ad})$. MSD is described by a power law of time over each of these intervals. In order to compute the total MSD (superposition), it is necessary to take first the logarithm such that the expression is rendered linear in time. Note that when all terms in (2) have power 1 (all chains are free), the product reduces to $\bar{t}$, as it should.

In order to obtain the behavior of the representative chain, it is necessary to average over all realizations of the random process q. This leads to

$$MSD(\bar{t}) = a^2 \frac{\bar{\tau}_{ad}}{N} \left\langle \prod_{j=1}^{\bar{t}/\bar{\tau}_{ad}} \left(\frac{(j+1)\bar{\tau}_{ad}}{j\bar{\tau}_{ad}} \right)^{q_j} \right\rangle =$$

$$= a^2 \frac{\bar{\tau}_{ad}}{N} \prod_{j=1}^{\bar{t}/\bar{\tau}_{ad}} \left\langle \left(\frac{(j+1)\bar{\tau}_{ad}}{j\bar{\tau}_{ad}} \right)^{q_j} \right\rangle \cong a^2 \frac{\bar{\tau}_{ad}}{N} \prod_{j=1}^{\bar{t}/\bar{\tau}_{ad}} \left(\frac{(j+1)\bar{\tau}_{ad}}{j\bar{\tau}_{ad}} \right)^{\langle q_j \rangle} \qquad (3)$$

The second equality holds because the process q is uncorrelated, while the third is an approximation which is based on Jensen's inequality [Hughes (1995) [10]: $\langle (1-p)^s \rangle \geq (1-p)^{\langle s \rangle}$ (where the random process is s, and $p < 1$). The approximation in eq. (3) carries the name of Rosenstock (1969) [29] who demonstrated that the left and the right hand side of the Jensen's inequality approach each other when p converges to 1 from below (which is the case here). It is also noted that the inequality follows from the relationship between the geometric and arithmetic means. Numerical studies indicate that, in the present case, the approximation is very good.

Hence, after using $\langle q \rangle = \phi_0$, the product in eq. (3) can be computed and the MSD results

$$MSD(\bar{t}) \cong a^2 \frac{\bar{\tau}_{ad}}{N} \left(\frac{\bar{t}}{\bar{\tau}_{ad}} \right)^{\phi_0}. \qquad (4)$$

It must be noted that out of the total population of chains only a fraction ϕ_0, those that are free at time zero, follow eq. (4). A fraction $\phi_0(1-\phi_0)$ become free for the first time after $\bar{t} = \bar{\tau}_{ad}$ and then follow eqn. (4) modified as $MSD(\bar{t}) \cong a^2 \frac{\tau_{ad}}{N} (\bar{t}/\bar{\tau}_{ad} - 1)^{\phi_0}$. In general, the chains that become free for the first time in the k-th time interval, at $\bar{t} = k\bar{\tau}_{ad}$, represent a fraction $\phi_0(1-\phi_0)^{k-1}$ of the population and their MSD is described by the equation

$$MSD(\bar{t}) \cong a^2 \frac{\bar{\tau}_{ad}}{N} (\bar{t}/\bar{\tau}_{ad} - (k-1))^{\phi_0}.$$

Moving to the limit of the continuous random walk, one may write the Chapman-Kolmogorov equation and derive the effective diffusion equation following the usual procedure. If $p(x, \bar{t})$ is the probability that the walker is found at position x (curvilinear along the chain) after normalized time $\bar{t}$ and neglecting convection, one has

$$p(x, \bar{t} + \bar{\tau}) \cong p(x, \bar{t}) - v\bar{\tau}^{\phi_0} \left. \frac{\partial p}{\partial x} \right|_{(x,\bar{t})} + \frac{\alpha}{2} \bar{\tau}^{\phi_0} \left. \frac{\partial^2 p}{\partial x^2} \right|_{(x,\bar{t})} \cdot \qquad (5)$$

Here, the effective "diffusion coefficient" $\alpha/2$ is $a^2\bar{\tau}_{ad}^{1-\phi_0}/N$ (which follows from (4)), and v is a drift velocity. The drift is considered to occur only when the chain is free. Otherwise the chain moves affinely with the mesh of entanglements.

Equation (5) leads to the following fractional convection-diffusion equation

$$\frac{\partial^{\phi_0} p}{\partial \bar{t}^{\phi_0}} = -v(x, \bar{t}) \frac{\partial p}{\partial x} + \frac{\alpha}{2} \frac{\partial^2 p}{\partial x^2}. \qquad (6)$$

The local fractional differential operator on the left hand side is defined as

$$\frac{\partial^{\phi_0} p}{\partial \bar{t}^{\phi_0}} = \lim_{\bar{\tau} \to 0} \frac{p(x, \bar{t} + \bar{\tau}) - p(x, \bar{t})}{\bar{\tau}^{\phi_0}}. \qquad (7)$$

This operator was introduced and its properties were studied by Kolwankar and Gangal (1998) [14] and Soare (2006) [32]. This maps the diffusion process from the real time to a fractional time with a support of fractal dimension ϕ_0. The fractional representation results here from the model and is not assumed. It can be shown that the solution of eq. (6) subject to the usual boundary conditions $p(s + L/2, \bar{t}) = p(s - L/2, \bar{t}) = 0$ (s denotes the position of a tube segment) and the initial condition $p(x,0) = \delta(x)$ [Doi and Edwards (1986) [6]], and under the assumption of

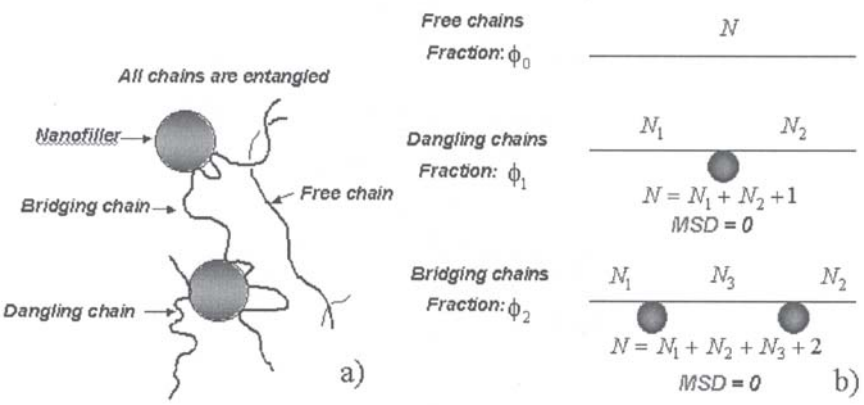

Fig. 1. a) Schematic representation of the nanocomposite molecular structure, b) The three types of chains considered in the model

time independent drift velocity v, is given by [Tikhonov and Samarskii (1963) [37]]

$$p(x,\bar{t}) = \left[\sum_{n=0}^{\infty}\frac{2}{L}\cos\frac{(2n+1)\pi s}{L}\cos\frac{(2n+1)\pi(s-x)}{L}\exp\left(-\frac{\alpha}{2}\frac{(2n+1)^2\pi^2}{L^2}\Im(\bar{t})\right)\right]\exp\left(\frac{vx}{\alpha}-\frac{v^2\Im(\bar{t})}{2\alpha}\right) \quad (8)$$

Here, $L=Na$ is the total chain length and $\Im(t)$ is the equivalent of the Devil Staircase function evaluated for a Cantor set of fractal dimension ϕ_0. If one measures the fractal with "a stick" of length τ_{ad} (which is the case in the present formulation), $\Im(t)$ is given by

$$\Im(\bar{t}) = \bar{\tau}_{ad}\left(\frac{\bar{t}}{\bar{\tau}_{ad}}\right)^{\phi_0}. \quad (9)$$

Hence, it follows that the MSD of eq. (4) is actually simply $MSD(\bar{t}) = a^2\,\Im(\bar{t})/N$, which must be compared with the usual equation for the mean square displacement of a free chain $MSD(\bar{t}) = a^2\,\bar{t}/N$.

This provides a transparent physical interpretation for the derivation. The motion of the representative chain may be viewed as the motion of a random walker on a temporal Cantor set of dimension ϕ_0 and the total time spent diffusing is equivalent with the effective length measured on the set with a stick of size τ_{ad}.

If the drift velocity cannot be considered constant over time $\bar{t}$, the convection-diffusion equation (6) must be solved numerically [Mead et al. 1995 [15], 1998 [17]]. Due to the fractional nature of the equation, its solution is time step dependent; the solution diverges as the time step decreases to zero. In order to preserve consistency with the formulation that led to eq. (6), one has to perform the integration with reference to $\bar{\tau}_{ad}$. This renders the solution unique.

The memory of the deformation at time zero preserved after time $\bar{t}$ is given by the fraction of chain segments that remain in the original tube. This can be computed using the usual procedure [Doi and Edwards (1986) [6]]. The probability of survival of the tube segment s at time is obtained by integrating eqn. (8) over x from $s-L/2$ to $s+L/2$:

$$\psi(s,\bar{t}) = \int_{s-Na/2}^{s+Na/2} p(x,\bar{t})\,dx, \quad (10)$$

while the fraction of segments surviving in the original tube results as the average of $\Psi(s,\bar{t})$ over the entire chain length:

$$f(\bar{t}) = \frac{1}{Na}\int_{-Na/2}^{Na/2}\psi(s,\bar{t})\,ds. \quad (11)$$

If ν can be considered time independent, an analytic form of the history-independent memory kernel can be derived from the solution (8). To this end, the drift velocity is pre-averaged and approximated as being linear in the curvilinear coordinate s [Ianniruberto and Marrucci (2000) [11]]. The memory function (and the relaxation) obtained by this procedure is a stretched exponential having a stretch power ϕ_0.

All results presented above pertain to a chain that starts as a free chain at time zero (e.g. onset of relaxation). However, only ϕ_0 of all chains is in this situation. The others become free at various moments of the system evolution, i.e. at times multiples of $\bar{\tau}_{ad}$. The fraction of chains that become free for the first time at $k\,\bar{\tau}_{ad}$ is given by $\phi_0(1-\phi_0)^k$. The MSD of a chain that becomes free at $k\,\bar{\tau}_{ad}$ is described by an equation identical to (4), except that the origin of t is shifted by $k\,\bar{\tau}_{ad}$. If v is a constant, one can write for these chains ${}^k f(\bar{t}) = f(\bar{t} - k\bar{\tau}_{ad})$.

Contour length fluctuations

All chains in the system perform contour length fluctuations at all times. However, every time a chain changes type, the length of the fluctuating arm changes. For example, if the chain is free, the arm length is half the chain length, $N/2$. When it is bridging or dangling, the length of the arm can take any value between 1 and N. This is described by the distribution function for the lengths N_1 and N_2 (fig. 1), function that has been evaluated by simulations [Ozmusul et al. (2005) [23]]. The probability distribution function (PDF) of the arm length for systems with large d ($d > 2R_g$) is almost constant, while for small d, it is biased toward the short segments.

The situation here is similar to that of star polymers. The nanoparticle carrying the dangling ends can be viewed as a star with multiple polydisperse arms. Contour length fluctuations in such systems (no detaching arms) is difficult to approach theoretically due to the complexity of dealing with constraint release. This problem has not been solved to date. However, theoretical results exist for the case of stars with monodisperse arms [Pearson and Helfand (1984) [25]; Milner and McLeish (1997) [18]]. The development here is based on these results.

The first passage time for the chain end retraction along the primitive path up to a distance r (the normalized version is $\bar{r} = r/a$) is viewed as a random walk in a potential defined by the chain configurational entropy component of the free energy, U_{eff}. If the length of the fluctuating arm is constant

during the observation time t, say N_i, the first passage condition reads $1 = f_{att}(N_i)\bar{t}\,exp\left(-\frac{U_{eff}(\bar{r},N_i)}{k_BT}\right)$, where f_{att} is the attempt frequency for chain retraction. This quantity can be taken as the inverse of the Rouse time of the respective dangling segment of length N_i, i.e. $f_{att} = 1/\tau_R(N_i a)$ Milner and McLeish (1997) [18] corrected the attempt frequency by a multiplicative factor.

In the case considered here, the number of segments of length a in the fluctuating segment, N_i, changes every $\bar{\tau}_{ad}$ and hence, for observation times $t >> \bar{\tau}_{ad}$, the first passage condition needs to be reformulated as,

$$1 = \sum_{i=1}^{\bar{t}/\bar{\tau}_{ad}} f_{att}(N_i)\bar{\tau}_{ad}\,exp\left(-\frac{U_{eff}(\bar{r},N_i)}{k_BT}\right). \quad (12)$$

The concept underlying eq. (12) is valid only if the attachment time is significantly larger than the inverse of the attempt frequency, $\bar{\tau}_{ad} > \bar{\tau}_R(N_i a)$. This condition is always fulfilled since only situations in which the attachment time is larger than the Rouse time of the entire chain $\bar{\tau}_R(Na)$ are considered.

The simplest and most physically transparent form of the effective potential U_{eff} is given by [Pearson and Helfand (1984) [25]]

$$U_{eff} = \frac{15}{8}\frac{\bar{r}^2}{N_i}. \quad (13)$$

However, this potential appears to be too stiff and predicts a very slow relaxation associated with arm retraction. An improved version that includes the effect of constraint release (dynamic dilution) was developed by Milner and McLeish (1997) [18] and reads

$$U_{eff} = \frac{27}{112}N_i\left[1-\left(1-\frac{\bar{r}}{N_i}\right)^{\frac{7}{3}}\left(1+\frac{7}{3}\frac{\bar{r}}{N_i}\right)\right] \quad (14)$$

This expression leads to an excellent match of experimental data and theoretical predictions for the relaxation of melts of star polymers or blends of linear and star polymers. Expression (14) reduces to (13) for small $\bar{r}$.

In order to account for all possible configurations, an average over N_i in eq. (12) is performed:

$$1 = \bar{t}\int_0^{N/2} f_{att}(N_i)\,exp\left(-\frac{U_{eff}(\bar{r},N_i)}{k_BT}\right)p(N_i)dN_i. \quad (15)$$

Here, $p(N_i)$ is the probability to find a dangling end of length N_i, quantity which was evaluated as a function of d and w by means of simulations [Ozmusul et al. (2005) [23]; Dionne et al. (2006) [4]]. This expression provides an implicit equation for $\bar{r}$ as a function of $\bar{t}$. It must be noted that this procedure neglects the speed-up of constraint release due to the polydispersity of the arm lengths. Nevertheless, some degree of constraint release is incorporated in (15) through the functional form of the potential (14) [Milner and McLeish (1997) [18]].

Chain stretch

Let us consider again a representative chain of the population. The chain becomes at random free, dangling or bridging. Stretch relaxes while the chain is dangling or free and cannot relax while the chain bridges two fillers (follows from the assumption of the affine motion of fillers). The stretch relaxation of the short dangling segments formed by a bridging chain is neglected. Hence, during relaxation, the representative chain stretch is enabled and disabled following a random sequence with characteristic time $\bar{\tau}_{ad}$. Let us describe this random process by a function of time, $H(\bar{t}, \xi)$, which is 0 if the chain is bridging, and is 1 if the chain is free or dangling. The stochastic parameter ξ describes the realization of the sequence, or the trajectory, i.e. for given ξ, H becomes a deterministic function of the normalized time. Further, a single mode stretch relaxation is considered, with the characteristic time being $\bar{\tau}_R(Na)$. The equation of evolution for the stretch λ becomes:

$$\dot{\lambda}(\bar{t},\zeta) = \lambda(\bar{t},\zeta) < v > (\bar{t}) - \frac{\lambda(\bar{t},\zeta)-1}{\bar{\tau}_R(Na)}H(\bar{t},\zeta). \quad (16)$$

The variable v represents the drift velocity imposed by the flow. The first term on the right hand side represents the imposed deformation, while the second one stands for relaxation. An approximation is made in (16) in that the stretch relaxation time is taken to be the Rouse time of the entire chain $\tau_R(Na)$ in all cases. The stretch relaxation time of a dangling segment of length $N_i < N$ is the Rouse time of the respective segment. Hence, the approximation leads to an overestimate of the stretch relaxation time.

If $p(\xi)$ is the probability for a chain to follow the trajectory defined by $H(\bar{t}, \xi)$, the average stretch at given time $\bar{t}$ is denoted as $\bar{\lambda}(\bar{t}) = \int p(\zeta)\lambda(\bar{t},\zeta)d\zeta$. Here the integral is performed over the phase space defined by ξ. Applying the averaging operator to eq. (16) leads to

$$\dot{\bar{\lambda}}(\bar{t}) = \bar{\lambda}(\bar{t}) < v > (\bar{t}) - \\ -\frac{1}{\tau_R(Na)}\left[\int\lambda(\bar{t},\zeta)p(\zeta)H(\bar{t},\zeta)d\zeta - \int p(\zeta)H(\bar{t},\zeta)d\zeta\right] \quad (17)$$

Let us consider now that all trajectories ξ are equally probable. Then, using the ergodicity property for the process, $H(\bar{t},\zeta)$, and $\int p(\zeta)H(\bar{t},\zeta)d\zeta = 1-\phi_2$, and $\int\lambda(\bar{t},\zeta)p(\zeta)H(\bar{t},\zeta)d\zeta = (1-\phi_2)\bar{\lambda}(\bar{t})$, and eq. (17) becomes

$$\dot{\bar{\lambda}}(\bar{t}) = \bar{\lambda}(\bar{t}) < v > (\bar{t}) - \frac{\bar{\lambda}(\bar{t})-1}{[\tau_R(Na)/(1-\phi_2)]}. \quad (18)$$

Hence, the relaxation remains exponential, but the characteristic time changes with the fraction ϕ_2 of bridging chains in the system.

Let us note that if a non-linear term in λ is used in the relaxation term of eqn. (16), e.g. by using the Warner approximation of the inverse Langevin function, an evolution equation of type (17) for the average of the stretch cannot be obtained anymore.

Stress evaluation

Let us consider a generic loading history for which the stress evolution must be evaluated in terms of the deformation history. Assuming that stress is due to both segment orientation, described by the orientation tensor $\bar{\mathbf{S}}(\bar{t})$, and stretch, and that one can use a multiplicative decomposition approximation, the stress tensor becomes:

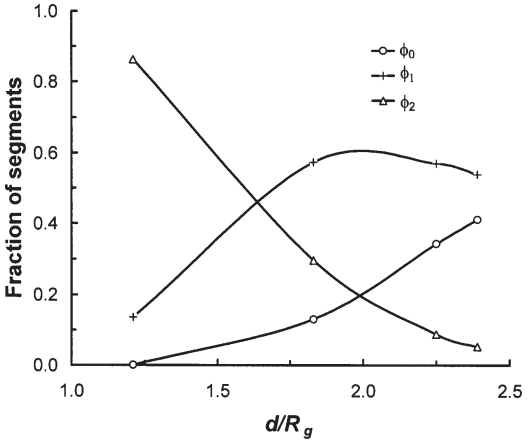

Fig. 2. Variation of the fraction of free, dangling and bridging chains with the normalized wall-to-wall distance, d/R_g. d measures the smallest wall-to-wall distance in a cubic packing of spherical fillers and R_g is the chain radius of gyration in the neat bulk polymer

System identifier	Fraction of free chains, ϕ_0	Fraction of dangling chains, ϕ_1	Fraction of bridging chains, ϕ_2
S1 (neat)	1	0	0
S2	0.5	0.5	0
S3	0.4	0.55	0.05
S4	0.23	0.56	0.21

Table 1

$$\boldsymbol{\sigma}(\bar{t}) = \frac{15}{4} G_0 \bar{\lambda}^2(\bar{t}) \bar{\mathbf{S}}(\bar{t}), \tag{19}$$

Where G_0 is the modulus and $\bar{\mathbf{S}}(\bar{t})$ is expressed as

$$\bar{\mathbf{S}}(\bar{t}) = -\int_{-\infty}^{\bar{t}} \left(\sum_{k=0}^{\infty} \phi_0 (1-\phi_0)^k \left[{}^k f(\bar{t},\bar{t}') \right] \right) \frac{d}{d\bar{t}'} \mathbf{Q}(\mathbf{E}(\bar{t},\bar{t}')) d\bar{t}'. \tag{20}$$

Here, $\mathbf{Q}$ is the Doi-Edwards tensor and $\mathbf{E}(\bar{t},\bar{t}')$ is the relative deformation gradient tensor between times $\bar{t}$ and $\bar{t}'$. The sum in eq. (20) reflects the fact that the average orientation of the chain segment population is computed as a weighted average over all chains in the system. The weights are $\phi_0(1-\phi_0)^k$, the fraction of chains that become free for the first time at $\bar{t}'+k\bar{\tau}_{ad}$, and ${}^k f(\bar{t},\bar{t}')$ represent the fraction of segments surviving at time $\bar{t}$ in the tube defined at time $\bar{t}'$. As discussed in Section 3.1, if v is a constant from $\bar{t}'$ to $\bar{t}$, one can write ${}^k f(\bar{t},\bar{t}') = f(\bar{t},\bar{t}'+k\bar{\tau}_{ad})$ for for $\bar{t} > \bar{t}'+k\bar{\tau}_{ad}$

Finally, for completeness, let us note that the relative tube-chain drift velocity is evaluated based on the average orientation tensor $\bar{\mathbf{S}}(\bar{t})$ and the velocity gradient $\mathbf{k}$ using the approximation of constant $\mathbf{S}$ along tube, as $\langle v(s,\bar{t}) \rangle = \boldsymbol{\kappa}(\bar{t}) : \bar{\mathbf{S}}(\bar{t}) s$

Numerical results and discussion

The behaviour of the model under various deformation conditions is discussed next. The emphasis is on identifying the influence of the various nanoscale parameters on the overall, material point mechanical behavior. Of primary interest are the wall-to-wall distance, d, and the polymer-filler affinity, w. These parameters are represented in the model through the fraction of free, dangling and bridging chains, and through the mean attachment time parameter $\bar{\tau}_{ad}$, respectively. As discussed in Section 2, the average lifetime of a polymer-filler contact, $\bar{\tau}_{ad}$, scales with the affinity w as $\exp(w/k_BT)$. The relationship between d and the three ϕ is more complicated and needs to be determined by simulations [Dionne et al. (2005) [3]]. Figure 2 [Dionne (2006) [5]] shows the variation of the three fractions with the normalized wall-to-wall distance d. The fraction of bridging and free chains are monotonic with d, while the fraction of dangling chains increases and then decreases with increasing d. This variation is due to the fact that at small d most dangling chains form bridges. The fractions are almost independent of w in the range of affinities studied (w = 1 … 8).

In this study, four systems are considered. Their ϕ values are given in table 1. S1 is the reference, neat polymer. S2 is a system with no bridges in which $d \sim 2.8\ R_g$. In this system the number of dangling chains per filler reaches saturation, i.e. is similar to that obtained for systems with very small filler volume fractions. The third system, S3, corresponds to $d = 2.4\ R_g$ and has a small fraction of bridging chains. The fourth system, S4, has a fairly large number of bridges per filler and corresponds to $d = 1.86\ R_g$ [Dionne (2005) [3]]. In the simulations performed by Dionne et al. (2005) [3], the polymer-filler affinity for systems S2-S4 was w = 1, i.e. neutral interactions. However, this parameter has a marginal effect on the structure.

Two types of flow are considered: relaxation following a step strain and a start-up shear flow. From the relaxation experiment one obtains the relaxation modulus, G(t) and the corresponding storage and loss moduli G' and G". In the shear flow case, the nature of the transient in the shear stress and the first normal stress difference, as well as their steady state values corresponding to various strain rates are analyzed. The various measures are evaluated based on the normalized stress $\hat{\boldsymbol{\sigma}}(\bar{t}) = \bar{\lambda}^2(\bar{t})\bar{\mathbf{S}}(\bar{t})$ (eq. (19)) and the time quantities are all normalized by the Rouse time of the entanglement segment, $\tau_R(a)$. The reference times are the Rouse time of the entire chain $\bar{\tau}_R(Na)$ and the disentanglement time $\bar{\tau}_d^{neat}$, both evaluated in the neat system. The equations of the model are integrated within the assumption of constant drift velocity v. Specifically, v is taken to be the average over the interval $\bar{t}'$ to $\bar{t}$. The approximation is good as one approaches the steady state of the constant rate deformation and less good during the start-up. Considering a constant drift velocity greatly simplifies the integration of the constitutive equation.

Figure 3 shows the relaxation modulus for the four systems. Here the curves were normalized by the value of the shear stress at the beginning of the relaxation period. The chain length considered was N = 20 entanglement segments and in all systems the mean attachment time was $\bar{\tau}_{ad} = 4\bar{\tau}_R(Na)$. The plot shows a significant slowing down of dynamics with decreasing wall-to-wall distance,

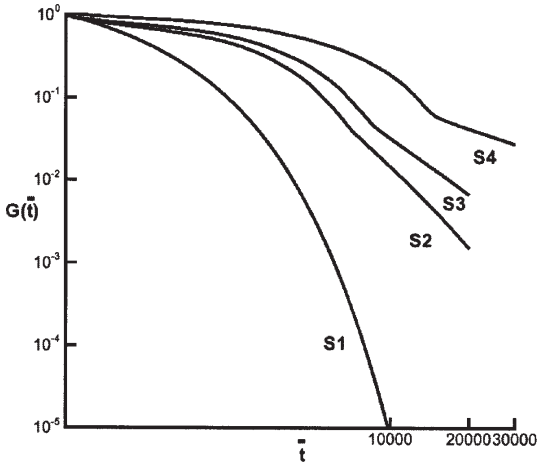

Fig. 3. Time dependence of the normalized relaxation modulus for systems S1, S2, S3 and S4 and for N = 20 and $\bar{\tau}_{ad} = 4\bar{\tau}_R(Na)$. The modulus is evaluated based on the normalized stress $\hat{\boldsymbol{\sigma}}(\bar{t}) = \bar{\lambda}^2(\bar{t})\bar{\mathbf{S}}(\bar{t})$ (eq. (19)) and is normalized by the value in the origin

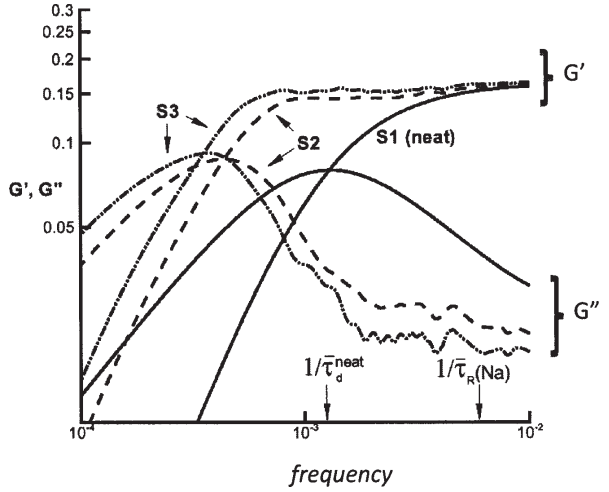

Fig. 4. Variation of the storage and loss moduli with the frequency (arbitrary units) for systems S1, S2 and S3 and for N = 20 and $\bar{\tau}_{ad} = 4\bar{\tau}_R(Na)$. The relaxation curves G(t) that led to these data have been shifted to start from the same value of stress. The modulus is evaluated based on the normalized stress $\hat{\boldsymbol{\sigma}}(\bar{t}) = \bar{\lambda}^2(\bar{t})\bar{\mathbf{S}}(\bar{t})$ (eq. (19))

or conversely, with increasing the filler volume fraction. Even the system S2 is affected by the slow down. Furthermore, all filled systems exhibit a two stage relaxation which is reminiscent of the two physical processes involved: disentanglement and attachment/ detachment.

Figure 4 shows the storage and loss moduli corresponding to the curves in figure 3. The curves for S1 are shown for reference. The right end of the frequency range of interest is $1/\bar{\tau}_R(Na)$. The rise of the curves at high frequency is not seen here because the Rouse modes are not included in the model. The only Rouse related relaxation is that of stretch, however, stretch is not activated in this small amplitude and relatively low rate loading. It is seen that the entanglement plateaus in the three systems are identical (after shifting) as observed in experiments [Zhu et al. (2005) [40]]. The attachment/detachment process leads to an extension of the G' plateau to lower frequencies. The plateau for S2 is lower than that for S3. Furthermore, the length of the plateau also depends on d (or filler volume fraction), a feature which is not immediately intuitive (as

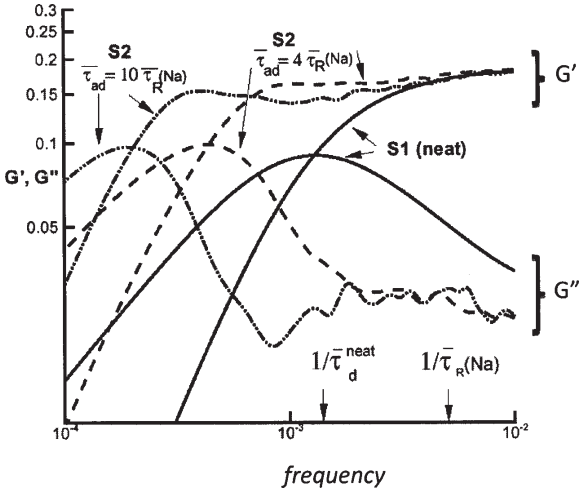

Fig. 5. Variation of the storage and loss moduli with the frequency (arbitrary units) for systems S1, S2 with N = 20, and for $\bar{\tau}_{ad} = 4\bar{\tau}_R(Na)$ and $\bar{\tau}_{ad} = 10\bar{\tau}_R(Na)$, representing an increase in polymer filler affinity. The modulus is evaluated based on the normalized stress $\hat{\boldsymbol{\sigma}}(\bar{t}) = \bar{\lambda}^2(\bar{t})\bar{\mathbf{S}}(\bar{t})$ (eq. (19))

the mean attachment time is the same in S2 and S3), but is observed in experiments.

It should be noted that making the attachment/ detachment characteristic time polydisperse, but preserving the mean, changes little in the qualitative features discussed here as long as the distribution of $\bar{\tau}_{ad}$ is symmetric with respect to the mean. Separate studies have shown that skewing the distribution towards short attachment times (which is the distribution shape suggested by the simulations of Dionne et al. (2006) [4]) leads to lowering or even eliminating the extension of the plateau at low frequencies. In these cases, the storage modulus decreases continuously with decreasing frequency just as for the neat polymer G', but at a lower rate than for S1. A similar behavior is seen in a purely frictional model of the nanocomposite in which the effect of the polymer-filler affinity is accounted for by increasing the effective monomeric friction coefficient [Sarvestani and Picu (2005) [31]]. In experiments it is seen that the secondary plateau in G' forms only at sufficiently large filler volume fractions [Sternstein and Zhou (2002) [36]]. At small filler volume fractions and with short chains, there is no plateau and G' decays continuously with decreasing frequency. G" follows the usual frequency dependence of the neat polymer, with the proper shift to lower frequencies as seen in G'.

The effect of the mean $\bar{\tau}_{ad}$ (or w) is demonstrated in figure 5, where G' and G" are shown for the system S2, for $\bar{\tau}_{ad} = 4\bar{\tau}_R(Na)$ and $\bar{\tau}_{ad} = 10\bar{\tau}_R(Na)$. Increasing the attachment time increases the length of the plateau in G' towards low frequencies, as expected, however, the plateau also sets at lower values. This effect does not appear to have been reported in experiments. In the context of this model, the decrease of the plateau level is due to the fact that, as $\bar{\tau}_{ad}$ increases, the relaxation of the chains that are free within given $\bar{\tau}_{ad}$ period is more pronounced. As $\bar{\tau}_{ad}$ increases, G" shifts to the left indicating an increase of the characteristic relaxation time of the system. The low amplitude features of G" at high frequencies and large $\bar{\tau}_{ad}$ are due to numerical inaccuracies in the integration of the equations in that range of frequencies.

The variation of the longest relaxation characteristic time τ_d with $\bar{\tau}_{ad}$ (or the polymer-filler affinity, w) is shown in figure 6. The time t_d is normalized by the disentanglement

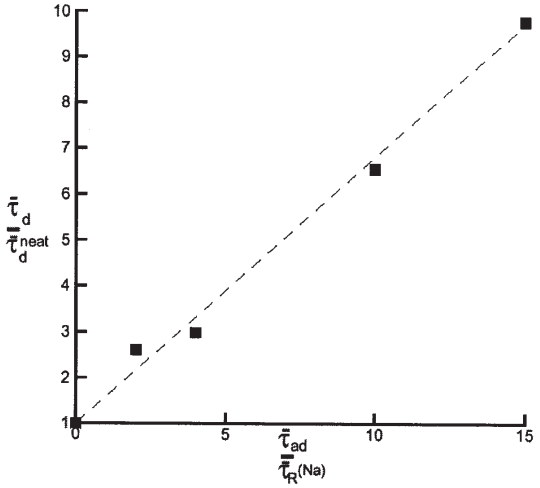

Fig. 6. Variation of the effective longest characteristic time of the system S2 with $\bar{\tau}_{ad} / \bar{\tau}_R(Na)$ representing increasing polymer-filler affinity. The longest characteristic time is obtained from figures 4 and 5. The dashed line is drawn to guide the eye.

time in the neat system, and τ_{ad} is normalized by the Rouse time of the entire chain. The relationship is essentially linear for the range of parameters studied. If the affinity w and the spatial range over which the polymer interacts energetically with the filler are significantly increased, a bound polymer layer is expected to form and hence the chain structure and the attachment/detachment process are expected to be different from those considered here. In such cases, the bound polymer layer effectively increases the radius of the filler, while the free chains do not interact with the filler, but rather with the like polymer chains and their tethered dangling ends that form the bound layer. The physics of this problem is slightly different and cannot be represented with the model in its current form.

Figures 7 and 8 show results for the start-up shear flow. Figure 7 shows the variation of the first normal stress difference $\hat{N}_1 = \hat{\sigma}_{11} - \hat{\sigma}_{22}$ and of the normalized shear stress $\hat{\sigma}_{12}$ with the strain (shear rate multiplied by normalized time) during the transient, for various rates and for system S3. The stretch-induced overshoot in $\hat{N}_1$ is observed for the highest Wissenberg number Wi (computed with respect to $\bar{\tau}_d^{neat}$), Wi = 4. Higher Wi number flows are expected to be influenced more significantly by hydrodynamic

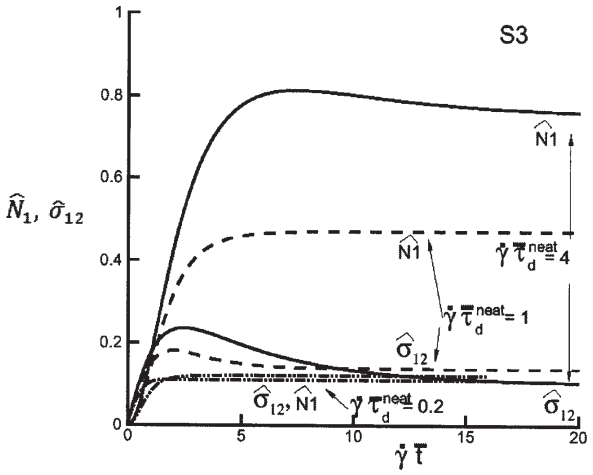

Fig. 7. Variation of the first normal stress difference $\hat{N}_1 = \hat{\sigma}_{11} - \hat{\sigma}_{22}$ and of the shear stress $\hat{\sigma}_{12}$ with strain during start-up shear flows of various shear rates. The normalized stress tensor $\hat{\mathbf{\sigma}}(\bar{t}) = \bar{\lambda}^2(\bar{t})\bar{\mathbf{S}}(\bar{t})$ is evaluated with eq. (19). The data are for system S3 with N = 20 and $\bar{\tau}_{ad} = 4\bar{\tau}_R(Na)$

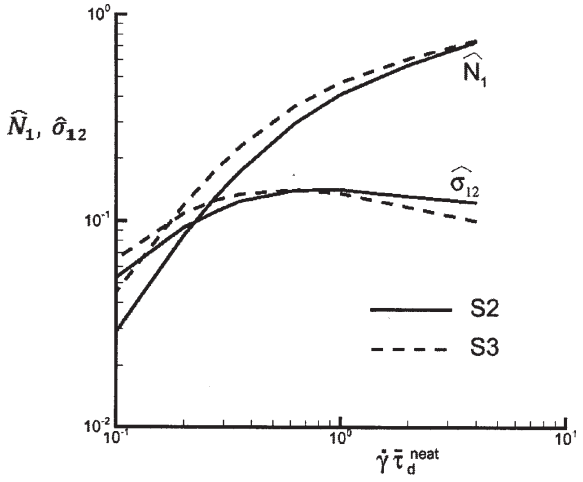

Fig. 8. Variation of the steady state normalized first normal stress difference $\hat{N}_1 = \hat{\sigma}_{11} - \hat{\sigma}_{22}$ and shear stress $\hat{\sigma}_{12}$ with strain rate for a simple shear flow. The normalized stress tensor $\hat{\mathbf{\sigma}}(\bar{t}) = \bar{\lambda}^2(\bar{t})\bar{\mathbf{S}}(\bar{t})$ is evaluated with Eq. (19). Data for systems S2 and S3 with N = 20 and $\bar{\tau}_{ad} = 4\bar{\tau}_R(Na)$ are shown

interactions involving filler particles, situations in which the present model provides only part of the stress. The effect of filling is to maintain the overshoot in the shear stress down to Wi numbers on the order of 1. Figure 8 shows the steady state dimensionless shear stress and first normal stress difference as a function of the shear rate. The decrease of the shear stress at high rates is attributed to the lack of convective constrain release [Mead et al. (1998) [17]]. At low rates, the plot exhibits the usual slopes that lead to constant shear/extensional viscosities. The two systems S2 and S3 exhibit the same qualitative behavior.

Conclusions

A constitutive model for the rheology of polymer nanocomposites was presented. The model accounts for relaxation due to chain reptation, contour length fluctuations and includes stretch. It accounts for the process of chain attachment/detachment to/from fillers and incorporates two parameters of the nanoscale problem. These are the filler wall-to-wall distance, which is related to the filler volume fraction, and an effective polymer filler affinity. Increasing both of these parameters leads to slowing down the relaxation and the extension of the relaxation plateau in the storage modulus towards low frequencies. The length of the plateau and the longest relaxation time in the system depend on both parameters. At higher frequencies, the model predicts the same entanglement-like plateau in both filled and neat systems. These features are also observed in experiments. The calibration of the model can be performed based on data for the neat polymer rheology, and based on discrete level simulations of the structure of the respective nano-composite system.

Acknowledgments: The authors thank P. Dionne and R. Ozisik for making available the fractions of the three types of chains in the filled systems studied (fig. 2).

References

1. BIRD, R.B., ARMSTRONG R.C., HASSAGER O., Dynamics of polymeric liquids, Vol. 2, Wiley, New York (1987).
2. CLANCY, T. C., MATTICE, W. L., "Role of the attractive portion of the Lennard-Jones potential in the homogeneity of melts of isotactic and syndiotactic polypropylene" J. Chem. Phys. **115**, 2001, p.8221-8225.

3. DIONNE, P.J., OZISIK, R., PICU, R.C., "Structure and dynamics of polyethylene nanocomposites," Macromolecules **38**,2005, p.9351-9358.
4. DIONNE, P.J., PICU, R.C., OZISIK, R., "Adsorption and desorption dynamics of linear polymer chains to spherical nanoparticles – a Monte Carlo study," Macromolecules **39**, 2006, p.3089-3092.
5. DIONNE, P.J., PH.D. Thesis, Rensselaer Polytechnic Institute, Troy, NY (2006).
6. DOI M., EDWARDS S.F., Theory of polymer dynamics, Clarendon, Oxford (1986).
7.FETTERS, L.J., LOHSE, D.J., MILNER, S.T., GRAESSLEY, W.W., "Packing length influence in linear polymer melts on the entanglement, critical, and reptation molecular weights" Macromolecules **32**, 1999, p.6847-6851.
8. GANESAN, V., PRYAMITSYN, V. "Entanglements in inhomogeneous polymeric phases" Macromolecules **35**, 2002, p.9219-9231.
9. GRAHAM, R.S., LIKHTMAN, A.E., MCLEISH, T.C. B., MILNER, S.T., "Microscopic theory of linear, entangled polymer chains under rapid deformation including chain stretch and convective constraint release," J. Rheol. **47**, 2003, p.1171-1200.
10. HUGHES, B.D., Random walks random environments, Vol. I, Clarendon Press, Oxford (1995).
11.IANNIRUBERTO, G. MARRUCCI, G., "Convective orientational renewal in entangled polymers," J. Non-Newt. Fluid Mech. **95**, 2000, p.363-374.
12.IANNIRUBERTO, G. MARRUCCI, G., "A simple constitutive equation for entangled polymers with chain stretch," J. Rheol. **45**, 2001, p.1305-
13. KAVASSALIS, T.A., NOOLANDI, J., "A new theory of entanglements and dynamics in dense polymer systems" Macromolecules **21**, 1988, p.2869-2879.
14.KOLWANKAR K.M., GANGAL, A.D., "Local fractional Fokker-Plank equation," Phys. Rev. Lett. **80**, 1998, p.214.
15.MEAD, D.W., LEAL, L.G., "The reptation model with segmental stretch I. Basic equations," Rheol. Acta **34**, 1995, p.339-359.
16. MEAD, D.W., YAVICH, D., LEAL, L.G., "The reptation model with segmental stretch, II. Steady flow properties," Rheol. Acta **34**, 1995, p.360-383.
17. MEAD, D.W., LARSON, R.G., DOI, M., "A molecular theory for fast flows of entangled polymers," Macromolecules **31**, 1998, p.7895-7914.
18. MILNER, S.T., MCLEISH, T.C.B., "Parameter-free theory for stress relaxation in star polymer melts" Macromolecules **30**, 1997, p.2159-2166.
19. MILNER, S.T., MCLEISH, T.C. B.. LIKHTMAN, A.E., "Microscopic theory of convective constraint release," J. Rheol. **45**, 2001, p.539
20. NG, C., SCHADLER, L. S., SIEGEL, R. W. "A study of the mechanical and premeability properties of nano-and micro-TiO2 filledepoxy composites," J. Nanostruct. Mater. **12**, 1999, p.507.
21.OZISIK, R., ZHENG, J., DIONNE, P. J., PICU, C. R., VON MEERWALL, E. D., "NMR relaxation and pulsed-gradient diffusion study of polyethylene nanocomposites," J. Chem. Phys. **123**, 2005, p.134901-1-8.
22. OZMUSUL, M.S., PICU, R.C., "Structure of polymers in the vicinity of convex impenetrable surfaces: the athermal case," Polymer **43**, 2002, p.4657-4665.
23.OZMUSUL, M.S., PICU, R.C., STERNSTEIN, S.S., KUMAR, S.K., "Lattice Monte Carlo simulations of chain conformations in polymer nanocomposites," Macromolecules **38**, 2005, p.4495-4500.
24. PAKULA, T., "Computer simulation in thin layers. I. Polymer melt between neutral walls - static properties" J. Chem. Phys. **95**, 1991, p.4685-4689.
25. PEARSON, D.S., HELFAND, E., "Viscoelastic properties of star-shaped polymers," Macromolecules **17**, 1984, p.888-895.
26. PICU, R.C., OZMUSUL, M.S., "Structure of linear polymer chains confined between impenetrable spherical walls," J. Chem. Phys. **118**, 2003, p.11239-11248.
27. PICU, R.C., RAKSHIT, A., "Dynamics of free chains in polymer nanocomposites," J. Chem. Phys. **126**, 2007, p.144909(1)-(6).
28. REICHERT, W.F., GORITZ, D., DUSCHL, E.J., "The double network, a model describing filled elastomers" Polymer **34**, 1993, p.1216-1221.
29. ROSENSTOCK, H.B., "Random walk on lattices with uncertain traps," SIAM J. Appl. Math. **27**, 1974, p. 457-463.
30. SARVESTANI, A.S., PICU, R.C., "Network model for the viscoelastic behavior of polymer nanocomposites," Polymer **45**, 2004, p.7779-7790.
31. SARVESTANI, A.S., PICU, R.C., "A frictional molecular model for the viscoelasticity of entangled polymer nanocomposites," Rheol. Acta **45**, 2005, p.132-141.
32. SOARE, M.A., "Mechanics of materials with hierarchical fractal structure," Ph.D. Thesis, Rensselaer Polytechnic Institute, Troy, NY (2006).
33. SHIMA, T., KUNI, H., OKABE, Y., DOI, M., YUAN, X.F., KAWAKATSU, T., "Self-consistent field theory of viscoelastic behavior of inhomogeneous dense polymer systems," Macromolecules **36**, 2003, p.9199-9204.
34. SMITH, G.D., BDEROV D., BORODIN O., "Structural relaxation and dynamic heterogeneity in a polymer melt at attractive surfaces," Phys. Rev. Lett. **90**, 2003, p.226103(1)-(4).
35. SMITH, K., VLADKOV M., BARRAT, J. L., "Polymer melt near a solid surface: a molecular dynamics study of chain conformations and desorption dynamics" Macromolecules **38**, 2005, p.571-580.
36. STERNSTEIN, S. S., ZHU, A., "Reinforcement mechanism of a nanofilled polymer melts as elucidated by nonlinear viscoelastic behavior" Macromolecules **35**, 2002, p.7262-7273.
37. TIKHONOV, A.N., SAMARSKII, A.A., Equations of mathematical physics, Dover,NewYork(1963)
38.ZHANG, Q., ARCHER, L., "Poly(ethylene oxide)/Silica nanocomposites: Structure and rheology" Langmuir **18**, 2002, p.10435-
39. ZHANG, Q., ARCHER, L., "Optical polarimetry and mechanical rheometry of poly(ethylene oxide)- silica dispersions" Macromolecules **37**, 2004, p.1928-1936.
40. ZHU, Z., THOMPSON, T., WANG, S. Q., VON MEERWALL E. D., HALASA, A., "Investigating linear and nonlinear viscoelastic behavior using model silica-particle-filled polybutadiene" Macromolecules **38**, 8816-8824 (2005).
41. WEI, L., TANG, T., HUANG, B., "Synthesis and characterization of polyethylene/clay-silica nanocomposites: A montmorillonite/silica-hybrid-supported catalyst and in situ polymerization" J. Polym. Sci., Part A **42**, 2004, p.941-949

Manuscript received: 7.05.2012